where $\tau = Dt/\delta^2$; D = diffusion coefficient of ionic species, cm.^{2} sec.$^{-1}$; t = time after current interruption, sec.; δ = effective boundary layer thickness (cm.); C_0 = initial concentration of ionic species (involved in the electrode reaction) at the electrode-electrolyte junction ($x = 0$) ; C = concentration of ionic species at $x = 0$, $t > 0$; C_b = bulk concentration of ionic species in electrolyte.

Equations 1 and 2 are re-arranged forms of solutions to related problems in heat conduction[1]. Equation 2 may be rendered in an alternative form which is useful for computation when τ is small, namely:

$$\frac{C - C_b}{C_0 - C_b} = 1 - 2\tau^{1/2} \sum_{n=0}^{\infty} (-1)^n \left\{ \frac{1}{\pi^{1/2}} e^{-n^2/\tau} - \right.$$
$$- \frac{n}{\tau^{1/2}} \left[1 - \operatorname{erf} \frac{n}{\tau^{1/2}} \right] - \frac{1}{\pi^{1/2}} e^{-(n+1)^2/\tau} +$$
$$\left. + \frac{n+1}{\tau^{1/2}} \left[1 - \operatorname{erf} \frac{n+1}{\tau^{1/2}} \right] \right\} \qquad (3)$$

For very small τ, equation (1) may be approximated as:

$$\frac{C - C_b}{C_0 - C_b} = 1 - \frac{2}{\pi^{1/2}} \tau^{1/2} \qquad (4)$$

Similarly, equation 3 may be reduced in form for small τ since all terms become zero for $n > 0$. The result is identical with equation 4. Thus, for small τ, the time behaviour of concentration at $x = 0$ is essentially independent of conditions at the outermost part of the boundary layer, that is, irrespective of the presence or absence of stirring.

Because of the equality of the solutions given by equations 1 and 2, 3 for small τ, it is suggested that this result may be utilized for the evaluation of boundary layer effective thickness in electrolytic systems. This may be accomplished by analysis of the decay of concentration polarization upon current interruption. By the Nernst relation:

$$\frac{C - C_b}{C_0 - C_b} = \frac{\exp[ZF\eta/RT] - 1}{\exp[ZF\eta_0/RT] - 1} \qquad (5)$$

where η_0 = concentration polarization at time zero; η = remaining polarization at $t > 0$; F = Faraday constant; R = gas constant; T = °K; Z = number of electrons in the electrode reaction. The approximation to equation 1 given in equation 4 is valid provided:

$$\operatorname{erf} \frac{1}{2\tau^{1/2}} \approx 1 \text{ and } e^{-1/4\tau} \approx 0$$

Arbitrarily choosing erf $1/2\tau^{1/2} = 0{\cdot}99$ yields an upper limit of $\tau = 0{\cdot}075$, whereas $e^{-1/4\tau} = 0{\cdot}01$ sets a limit of $\tau = 0{\cdot}054$. Taking a limit of $\tau = 0{\cdot}05$ together with $D = 10^{-5}$ cm.^{2}/sec., it may readily be seen that for the very thin boundary layers encountered in stirred systems ($\delta \approx 10^{-3}$ cm.), the overvoltage measuring device should be able to resolve time to better than 5 msec., suggesting an oscilloscopic technique. For thicknesses of about 0·5 mm., encountered in natural convexion systems, time resolution need only be better than about 10 sec., which is well within the range of chart recorders.

In the dimensionless time $\tau = 0{\cdot}05$, the concentration (activity) fraction has dropped from unity to about 0·75. The fractional decay of polarization depends on the initial value before current interruption, according to equation 5. At 25° C. and for $z = 2$, an initial polarization of 30 mV. will have decayed to about 14·6 mV. in the interval $0 < \tau < 0{\cdot}05$. From the relationship of equation 5 with equations 1–4, it is clear that for any hydrodynamic conditions, such as stirring or its absence, all anode concentration polarization data can be normalized according to equation 5 and fitted to a master curve (equation 4) provided the real time-scale (in sec.) is multiplied by D/δ^2. Since D is generally known, a graphical method may be used to cause a plot of the function of η, η_0 given in equation 5 versus time to be superimposed on a master plot the abscissa of which is rendered in dimensionless time τ, such as that given by equation 4 for $0 < \tau < 0{\cdot}05$.

From equation 4, it may be seen that the time required to attain a given fractional decay varies as the square of the boundary layer thickness δ, indicating that the proposed graphical method will permit a good resolution of the actual magnitude of δ. Equations 1–4 may also prove useful as a means for separating concentration polarization from other types of overvoltage.

Work is in progress to prepare analytical solutions similar to equations 1 and 2 for a concentration contour which is better than the linear approximation for actual systems. Functional tables for equations 1 and 2 over a wide range of τ and tables of the general term of equation 5 are in preparation.

This work was supported by the U.S. Office of Naval Research.

Leonard Nanis

Stanley-Thompson Laboratories,
Henry Krumb School of Mines,
Columbia University,
New York 27.

[1] Carslaw, H. S., and Jaeger, J. C., *Conduction of Heat in Solids*, 54, 97 (Oxford Univ. Press, 1959).

Pyrolytic Carbon Formation from Carbon Suboxide

Almost all the extensive work done on the formation of pyrolytic carbon films has consisted of the decomposition of a hydrocarbon on non-metallic substrates like porcelain or artificial graphite. Work is in progress in our laboratory investigating the kinetics and mechanism of carbon film formation on glazed porcelain from carbon suboxide (C_3O_2)[1]. In the course of this work, it was of interest to look briefly, initially, at the effect of some different substrates on the qualitative rate of carbon formation and more particularly on the nature of the film formed.

Very pure C_3O_2, entrained in pre-purified helium, was pyrolysed at 713° C. for about 3 hr. over porcelain, electrolytic nickel and copper foils, and reagent grade platinum foils. The concentration of C_3O_2 at the pyrolysis temperature was about 6×10^{-6} mole/l. Tenacious and hard carbon films were obtained, with the rate of film formation on nickel being roughly four times that on the other substrates.

The carbon films were separated from the metal substrates by acid treatment prior to studying their structure by transmission electron diffraction and

Table 1. Spacings of (*hkl*) Lines of Film Carbon deposited from C_3O_2 on to a Nickel Substrate at 713° C.

(*hkl*) Graphite	d_g, A	d_{fc}, A	Intensity of experimental halos
002	3·370	3·370	medium
100	2·102	2·091	broad ring with very strong intensity
101	2·036		
110	1·232	1·230	very strong
112	1·150	1·155	strong
200	1·063	1·060	medium
210	0·804	0·799	medium
310	0·709	0·704	medium

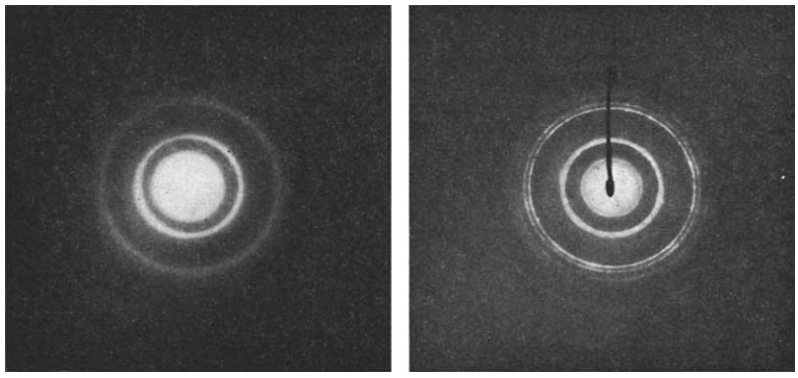

a *b*

Figs. 1 *a* and *b*. Transmission electron diffraction patterns of film carbon deposited from C_3O_2 on to a substrate at 713° C.; *a*, copper substrate; *b*, nickel substrate

transmission electron microscopy. 50-kV. electrons, having a beam width of 10μ, were used. Fig. 1 (*a*) shows the diffraction pattern for the film carbon resulting from deposition over a copper substrate. Diffuse halos, corresponding to the (10) and (11) reflexions of a polycrystalline, turbostratic carbon[2], are observed. The absence of a strong (002) reflexion when the incident electron beam is normal to the film surface is indicative of preferred orientation of the basal planes parallel to this surface. Diffraction patterns very similar to Fig. 1*a* were obtained from the film carbon deposited on a porcelain or platinum substrate.

On the other hand, the diffraction pattern (Fig. 1*b*) of the film carbon deposited on the nickel substrate is characteristic of a material of substantial crystallite size, in which the crystallites have extensive three-dimensional ordering. Table 1 compares the *d*-spacings for the film carbon (d_{fc}) with comparable spacings calculated from the graphite lattice (d_g). Similar diffraction patterns for carbon films deposited on porcelain, copper, or platinum are obtained only when the separated films are ultimately heated in excess of 2,000° C.

Fig. 2 is an electron micrograph of the carbon film deposited on nickel. Variations in the thickness of the films are evident. In addition, the presence of small, white circular spots is noted. It is suggested that these spots were formed by the removal by acid treatment of inclusions of nickel and/or nickel carbide which were originally present, but this has not been verified. From work on the interaction of evaporated carbon films with a similar nickel substrate on subsequent heat treatment, it is known that substantial inter-diffusion of nickel and carbon occurs at 500° C. and above (Banerjee, B. C., and Walker, P. L., unpublished results).

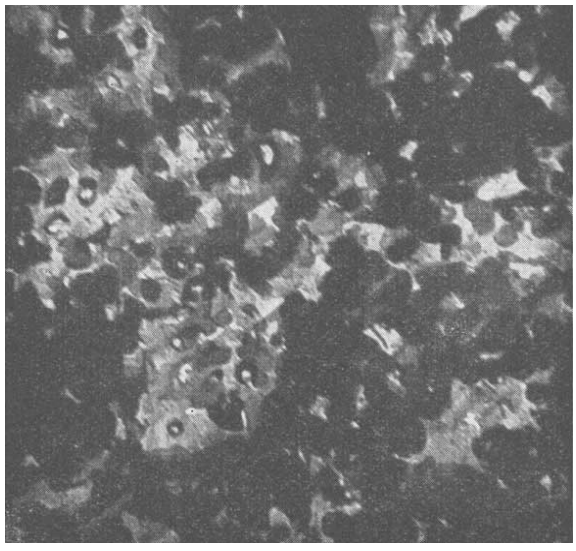

Fig. 2. Transmission electron micrograph of film carbon deposited from C_3O_2 on to a nickel substrate at 713° C. (× *c.* 4,700)

These results clearly suggest that more attention might be paid to the effect of the substrate in work on the formation of pyrolytic carbon films. In particular, substrates of nickel and iron are of interest. They are highly active catalysts for the decomposition of carbonaceous gases, apparently because of the incomplete filling of their 3*d* bands. In addition, they markedly increase the crystallinity of the carbon formed as a decomposition product. The effect of nickel is clearly evident from this work. The effect of iron, both on rate of formation and structure of carbon, has been previously shown for carbon monoxide decomposition[3].

We thank the Atomic Energy Commission, contract No. *AT*(30–1)–1710, for support of this work.

B. C. Banerjee
T. J. Hirt
P. L. Walker, jun.

Fuel Technology Department,
The Pennsylvania State University,
University Park, Pennsylvania.

[1] Hirt, T. J., and Palmer, H. B., *Abstr. Fifth Biennial Conf. Carbon*, 9 (June 19–23, 1961).
[2] Biscoe, J., and Warren, B. E., *J. App. Phys.*, **13**, 364 (1942).
[3] Walker, jun., P. L., Rakszawski, J. F., and Imperial, G. R., *J. Phys. Chem.*, **63**, 133, 140 (1959).

BIOCHEMISTRY

Changes in Adenine Nucleotides in the Muscles of Some Marine Invertebrates

Hitherto it has been generally accepted that most vertebrate muscles contain an enzyme specific for the deamination of 5′-adenylic acid (AMP) which is formed principally from adenosine triphosphate (ATP). On the other hand, in the case of invertebrates the presence of such an enzyme has been questioned[1].

Recently we have studied the changes in adenine nucleotides in the muscles of some marine invertebrates (prawn, squill, crab, squid, and some sea shells), and observed that those of prawn, squill, and crab contain certain amounts of 5′-inosinic acid (IMP) in addition to AMP, while in others AMP alone is accumulated.

Chopped muscles of each animal were stored in a glass-covered dish at an ambient temperature of − 5° C. in order to minimize bacterial effects. Two gm. of muscle were ground by hand in a mortar in 20 ml. of cold, 4 per cent perchloric acid solution. The extract was filtered and 10 ml. of the filtrate were used for